JOURNAL OF MATERIALS SCIENCE 20 (1985) 2323–2334

Correlation between structural relaxation enthalpy and superconducting properties of amorphous $Zr_{70}Cu_{30}$ and $Zr_{70}Ni_{30}$ alloys

A. INOUE, K. MATSUZAKI*, N. TOYOTA, H. S. CHEN‡, T. MASUMOTO, T. FUKASE
The Research Institute for Iron, Steel and Other Metals, Tohoku University, Sendai 980, Japan

The anneal-induced change in the superconducting properties together with the irrecoverable relaxation enthalpy ($\Delta H_{i,exo}$) and recoverable relaxation enthalpy ($\Delta H_{r,endo}$) of amorphous $Zr_{70}Cu_{30}$ and $Zr_{70}Ni_{30}$ alloys was examined. The increase in $\Delta H_{i,exo}$ and the degradation of T_c progress logarithmically with annealing time t_a in a temperature range of 373 to 523 K. The activation energy and the attempted frequency were respectively estimated to be 1.5 eV and $6.6 \times 10^{13}\,sec^{-1}$ for the increase in $\Delta H_{i,exo}$ and 1.5 eV and $1.9 \times 10^{14}\,sec^{-1}$ for the degradation of T_c. The recoverable structure relaxation exerts little effect on T_c. Based on the agreement between the kinetic parameters for the changes of $\Delta H_{i,exo}$ and T_c, it appears that the degradation of T_c on annealing is associated with the irrecoverable structural relaxation as a result of the annihilation of frozen-in defects and the topological and compositional atomic rearrangement. The values of the attempted frequency being of the order of Debye frequency suggest that the irrecoverable structural relaxation processes occur more or less independently from each other. The dressed density of electronic states at the Fermi level, $N(E_f)(1 + \lambda)$, determined from the measured values of ρ_n and $-(dH_{c2}/dT)_{T_c}$ using GLAG (theory), was found to have a similar annealing dependence to that of T_c. The degradation of T_c by the irrecoverable relaxation was thus inferred as resulting from the decrease in λ due to the decrease in $N(E_f)$ and the increases in M and ω. Furthermore, the irrecoverable structural relaxation resulted in a significant depression of fluxoid pinning force and was interpreted as due to an enhanced structural homogeneity on the scale of coherence length.

1. Introduction

When an amorphous alloy prepared by liquid quenching is subjected to heat treatments well below the glass transition temperature T_g, irrecoverable and recoverable structural relaxations take place, leading to the changes in various physical and thermodynamical properties. For instance, the superconducting transition temperature T_c has been reported to be lowered upon annealing for a number of amorphous superconducting alloys such as Zr–Rh [1], Zr–Ni [2], Zr–Cu [3], Mo–Ru–B [4], Zr–Si [5] and Nb–Zr–Si [5], etc. However, there is no information regarding the correlation between the anneal-induced change in the superconducting properties such as T_c, upper critical magnetic field $H_{c2}(T)$

*Department of Metallurgy, Graduate School, Tohoku University.
‡ATT Bell Laboratories, Murray Hill, New Jersey 07974, USA.

and critical current density $J_c(H)$, and the amount of irrecoverable and recoverable structural relaxation. Since the irrecoverable and recoverable structural relaxation have been inferred [6] as arising from a topological short-range ordering and a compositional short-range ordering, respectively, a distinguishing of the contribution of the two structural relaxations on the superconducting characteristics is of a vital interest. This paper examines the changes in the superconducting properties of T_c, $H_{c2}(T)$ and $J_c(H)$ and the thermodynamic parameters of specific heat and enthalpy upon structural relaxation for $Zr_{70}Cu_{30}$ and $Zr_{70}Ni_{30}$ amorphous alloys subjected to various heat treatments below T_g, and investigates the correlation between the anneal-induced change in the superconducting properties and the structural relaxation. The Zr–Cu alloy is of particular interest as it is the only amorphous alloy system which is known to exhibit both superconductivity and glass transition phenomenon. It offers us a unique opportunity of interpreting quantitatively the effect of structural relaxation on the superconducting properties of amorphous alloys.

2. Experimental methods

The materials used in the present work are $Zr_{70}Cu_{30}$ and $Zr_{70}Ni_{30}$ amorphous ribbons having about 20 μm thickness and about 1.5 mm width. The amorphous ribbons were produced in argon atmosphere by the single-roller melt spinning method and the amorphous nature of the as-quenched ribbons was confirmed by the diffractometer X-ray method using Cu*Kα* radiation combined with an X-ray monochrometer as well as transmission electron microscopy.

The changes in the superconducting and electrical properties and the temperature dependence of specific heat $C_p(T)$ upon annealing were examined on specimens annealed for the periods of $t_a = 1$, 10 and 100 h at different temperatures in the range of 373 to 523 K in evacuated quartz capsules. Measurements of superconducting properties T_c, $J_c(H)$ and $H_{c2}(T)$ were made by the d.c. method using the four electrical probes and the a.c. susceptibility method using a Hartshorn bridge. The temperature was measured with an accuracy of ± 0.01 K using a calibrated germanium thermometer. A magnetic field of up to 9 T was applied perpendicular to the specimen surface and feed current. In addition, measurement of the normal electrical resistivity $\rho(T)$ was made in the temperature range from 77 to 250 K by the four-electrical-probe method and the temperature was measured with an accuracy of ± 0.1 K using a calibrated diode thermometer.

The $C_P(T)$ was measured with a differential scanning calorimeter (Perkin-Elmer DSC-II). The sample was thermally scanned at 40 K min^{-1} from 320 to 645 K for $Zr_{70}Cu_{30}$ and 630 K for $Zr_{70}Ni_{30}$ to determine the $C_p(T)$ of the as-quenched and annealed state. It was then cooled to 320 K, and reheated immediately to obtain the $C_{p,s}(T)$ data of the "reference" sample. The change in the calorimetric behaviour with annealing was used to monitor the amount of structural relaxation. The accuracy of the data was about 0.8 J mol^{-1} K^{-1} for the absolute C_p values, but was better than 0.4 J mol^{-1} K^{-1} for the relative C_p or ΔC_p measurement.

3. Results

3.1. Change in $C_p(T)$ behaviour on annealing

Figs. 1 to 3 show the change in the thermograms of $Zr_{70}Cu_{30}$ amorphous samples with annealing at T_a = 373, 423, 473 and 523 K for t_a = 1, 10 and 100 h, respectively. The C_p value of the as-quenched sample is about 26.2 J mol^{-1} K^{-1} near room temperature, being almost the same as those of a number of metal–metalloid type amorphous alloys [7–10]. On subsequent heating, the C_p value begins to decrease indicative of a structural

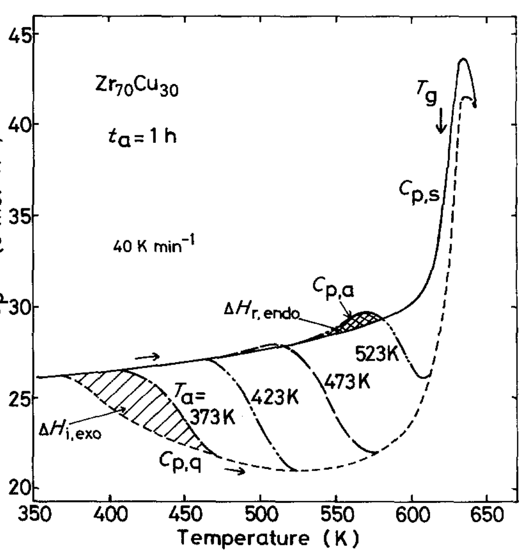

Figure 1 The thermograms of an amorphous $Zr_{70}Cu_{30}$ alloy subjected to anneals for 1 h at various temperatures from 373 to 523 K.

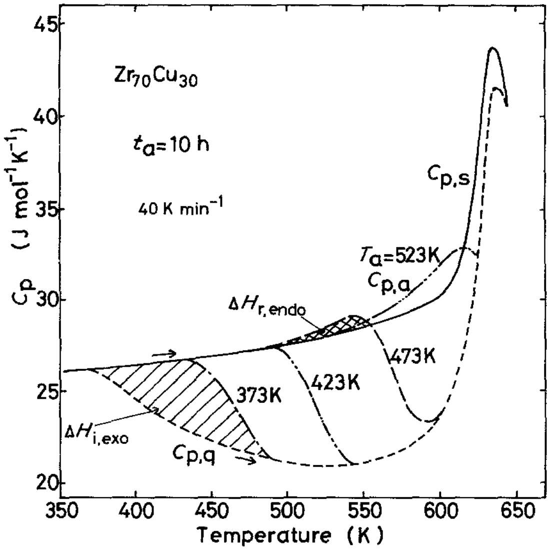

Figure 2 The thermograms of an amorphous $Zr_{70}Cu_{30}$ alloy subjected to anneals for 10 h at various temperatures from 373 to 523 K.

relaxation at about 368 K and shows a minimum value of about 20.8 J $mol^{-1}K^{-1}$ in the vicinity of 530 K. With further rising temperature, C_p increases gradually up to about 600 K and then rapidly, indicative of a glass transition. The C_p of both the as-quenched ($C_{p,q}$) and the reference ($C_{p,s}$) sample approaches the equilibrium liquid values above

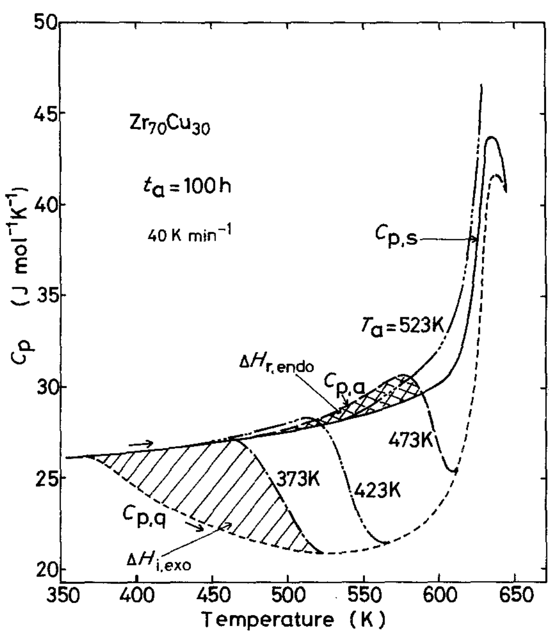

Figure 3 The thermograms of an amorphous $Zr_{70}Cu_{30}$ alloy subjected to anneals for 100 h at various temperatures from 373 to 523 K.

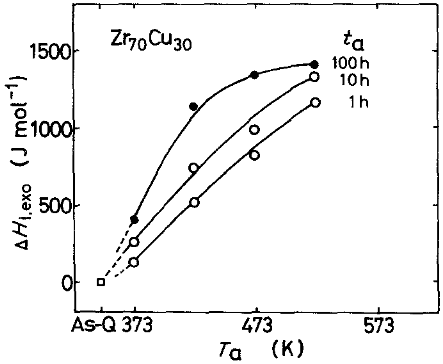

Figure 4 Change in the irrecoverable relaxation enthalpy as a function of annealing temperature (T_a) for an amorphous $Zr_{70}Cu_{30}$ alloy annealed for 1, 10 and 100 h.

644 K. Such a $C_p(T)$ behaviour of the $Zr_{70}Cu_{30}$ amorphous alloy is very similar to the previous results [7–11] for a number of amorphous alloys. The $C_p(T)$ curves of the samples annealed at temperatures below 423 K for 1 and 10 h and below 373 K for 100 h reveal only a broad exothermic peak, whereas those of the samples annealed at higher temperatures closely follow the $C_{p,s}$ curve up to each annealing temperature, and then exhibit an excess endothermic peak relative to the reference sample before the appearance of a broad and large exothermic peak. The exothermic broad peak is irrecoverable while the excess endothermic peak is recoverable. It has been interpreted [7–11] that the recoverable relaxation arises from compositional short-range localized relaxation in regions of the more or less rigid matrix while the irrecoverable structural relaxation results from the annihilation of various kinds of quenched-in "defects" as well as the topological and compositional atomic regroupings.

The area marked with oblique lines in Fig. 1 represents the amount of irrecoverable structural relaxation during annealing for 1 h at 373 K and is expressed by

$$\Delta H_{i,exo} = \int \Delta C_p (= C_{p,a} - C_{p,q}) dT \quad (\Delta C_p \geqslant 0) \tag{1}$$

The $\Delta H_{i,exo}$ values for $Zr_{70}Cu_{30}$ amorphous alloy annealed for t_a at T_a are plotted as a function of T_a in Fig. 4. The $\Delta H_{i,exo}$ increases significantly with increasing T_a and t_a and the annealing for 100 h at 523 K results in a saturated value of about 1400 J mol^{-1}, indicating that the topological structure relaxation due to the annihilation of quenched-in "defects" and the atomic regrouping

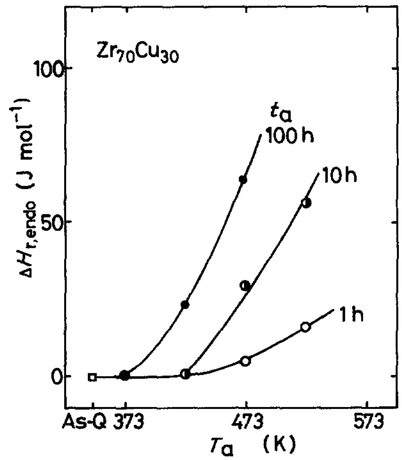

Figure 5 Change in the recoverable relaxation enthalpy as a function of annealing temperature (T_a) for an amorphous $Zr_{70}Cu_{30}$ alloy annealed for 1, 10 and 100 h.

is nearly complete. The endothermic enthalpy corresponding to the area marked with double oblique lines is given by

$$\Delta H_{r,endo} = \int \Delta C_p (= C_{p,a} - C_{p,s}) dT \quad (\Delta C_p \geqslant 0) \tag{2}$$

Fig. 5 shows the $\Delta H_{r,endo}$ values as a function of T_a. The $\Delta H_{r,endo}$ increases with increasing T_a and t_a. It is about 59 J mol^{-1} after annealing for 10 h at 523 K, being smaller by a factor of about 25 than the $\Delta H_{i,exo}$ values, however, the $\Delta H_{r,endo}$ is not in saturation even after t_a = 100 h at 523 K.

3.2. Change in T_c upon annealing

Fig. 6 shows the change in the reduced resistance in the temperature range near T_c for $Zr_{70}Cu_{30}$ amorphous alloy with T_a for t_a = 1 h. With rising T_a, T_c lowers from 2.69 K in the as-quenched state to 2.26 K for the fully relaxed state. Further, it is noticed that the transition width from the normal to superconducting state decreases initially with T_a, and attains a minimum value ($\simeq$ 0.01 K) at T_a = 423 and 473 K. It then increases with further increase in T_a. Fig. 7 shows the change in T_c of $Zr_{70}Cu_{30}$ and $Zr_{70}Ni_{30}$ amorphous alloys with T_a and t_a. Here T_c is defined as the temperature corresponding to $R/R_n = 0.5$, where R_n is the resistance in the normal state. T_c degrades definitely on annealing and the degradation is greater in the temperature range below 423 K. The annealing condition where T_c becomes saturated is T_a = 523 K and t_a = 100 h for $Zr_{70}Cu_{30}$ alloy, in good agreement with that in which the increase in the $\Delta H_{i,exo}$ is saturated. The saturated T_c value of the fully relaxed amorphous alloy is 2.24 K for $Zr_{70}Cu_{30}$ and 2.78 K for $Zr_{70}Ni_{30}$, which are independent of the previous thermal conditions.

3.3. Change in T_c upon recoverable structural relaxation

In the previous subsection (3.1), it was shown that the irrecoverable structural relaxation causes a degradation of T_c and the degradation ratio reaches 17% for $Zr_{70}Cu_{30}$ and 12% for $Zr_{70}Ni_{30}$. We examined here the change of T_c upon the recoverable structural relaxation. Fig. 8 illustrates the annealing process which was performed for $Zr_{70}Cu_{30}$ amorphous alloy in order to examine the influence of the recoverable structural relaxation on T_c. The "A" treatment results in a completion of the irrecoverable structural relaxation. On a subsequent treatment "A + B" a recoverable short-range ordering develops in the topologically

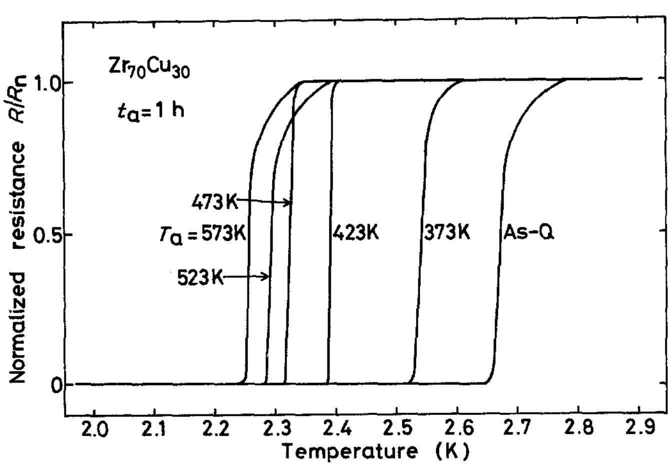

Figure 6 Change in the normalized electrical resistance R/R_n as a function of temperature for an amorphous $Zr_{70}Cu_{30}$ alloy annealed for 1 h at various temperatures from 373 to 573 K.

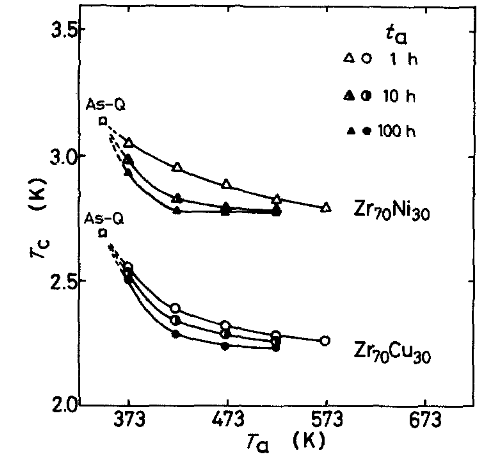

Figure 7 Change in the superconducting transition temperature T_c as a function of annealing temperature for amorphous $Zr_{70}Cu_{30}$ and $Zr_{70}Ni_{30}$ alloys annealed for various periods from 1 to 100 h.

relaxed amorphous phase and a further treatment "C" results in an annihilation of the short-range ordering which developed during the "A + B" treatment, and leads to the same amorphous structure as that after the "A" treatment.

Fig. 9 shows the change in the a.c. susceptibility (χ') in the temperature range near T_c for $Zr_{70}Cu_{30}$ amorphous samples on each treatment of "A", "A + B" and "A + B + C". Here T_c was defined as the temperature where the straight line extrapolated from the saturated part of χ' intersects that from the rapidly increasing part of χ'. As seen in the figure, T_c is 2.63 K for the as-quenched state and decreases to 2.22 K on the "A" treatment. The T_c value is almost equal to that (2.23 K) of the sample in which the irrecoverable relaxation was complete upon annealing for $t_a = 100$ h at $T_a = 523$ K. The T_c value of the sample subjected to the "A + B" treatment is also 2.22 K and remains unchanged in spite of the development of short-range ordering. In addition, the T_c exhibits a nearly constant value (2.26 K) after the annihilation of the short-range ordering by the "A + B + C" treatment. Thus there is no detectable change in T_c by the development of recoverable short-range ordering and it is therefore concluded that the degradation of T_c on annealing arises from the development of topological and compositional short-range ordering caused by the irrecoverable structural relaxation. This conclusion is also supported from the results shown in Figs. 3 and 7 that the T_c value (2.24 K) of the sample annealed at 523 K for 100 h, in which the irrecoverable structural relaxation was complete and only the recoverable compositional ordering developed significantly, is almost equal to those (2.22 or 2.26 K) of the samples subjected to the "A" or "A + B + C" treatment.

3.4. Change in $H_{c2}(T)$ upon annealing

Fig. 10 shows the temperature dependence of H_{c2} near T_c for $Zr_{70}Cu_{30}$ amorphous alloy annealed for 1 h at different temperatures ranging from 373 to 573 K. The solid lines represent a linear relation of $H_{c2}(T)$ near T_c. It is seen that H_{c2} near T_c increases linearly with lowering temperature. The $-(dH_{c2}/dT)_{T_c}$ values of $Zr_{70}Cu_{30}$ amorphous alloy annealed for $t_a = 1$, 10 and 100 h are shown as a function of T_a in Fig. 11. The gradient is $2.60\,T\,K^{-1}$ in the as-quenched state and decreases with increasing T_a and t_a, i.e. $2.45\,T\,K^{-1}$ for 10 h at 473 K and $2.40\,T\,K^{-1}$ for 100 h at 523 K.

3.5. Change in fluxoid pinning force upon annealing

Fig. 12 shows the magnetic field dependence of J_c at 1.40 K for $Zr_{70}Cu_{30}$ amorphous alloy in the as-quenched and annealed states for 1 h at 373 and 473 K. Annealing causes a significant depression of $J_c(H)$ values and the depression increases with rising T_a. Such a tendency agrees well with the

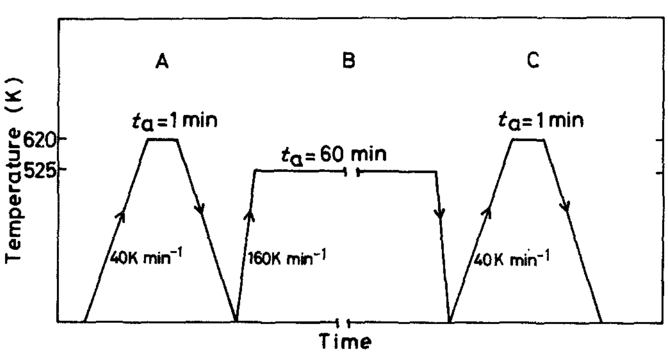

Figure 8 Schematic diagram of the annealing treatments leading to the generation and disappearance of the recoverable structural relaxation for an amorphous $Zr_{70}Cu_{30}$ alloy.

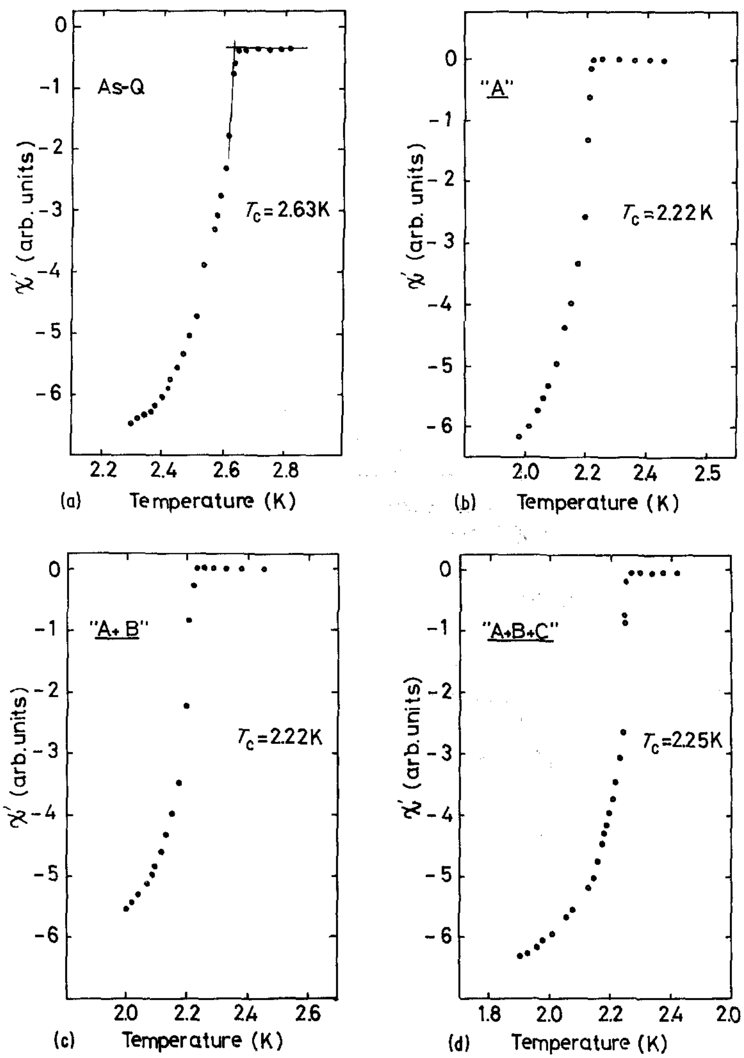

Figure 9 Temperature dependence of a.c. susceptibility for an amorphous $Zr_{70}Cu_{30}$ alloy subjected to the annealing treatments shown in Fig. 8.

previous results [4, 5] for Mo–Ru–B, Nb–Zr–Si and Zr–Si amorphous alloys. This indicates that the fluxoid pinning force in the amorphous phase becomes weaker with proceeding irrecoverable structural relaxation. Since the depression of $J_c(H)$ on annealing shown in Fig. 12 is considered to reflect the lowering of T_c and H_{c2}, the fluxoid pinning force F_p as a function of magnetic field B/H_{c2} was plotted in Fig. 13, where F_p is calculated by $B \times J_c$. The maximum F_p at 1.40 K is about $2.5 \times 10^4\,N\,m^{-3}$ in the as-quenched state and decreases with increasing T_a, i.e. about $1.2 \times 10^4\,N\,m^{-3}$ at $T_a = 373\,K$ and about $0.9 \times 10^4\,N\,m^{-3}$ at $T_a = 473\,K$. The value of B/H_{c2} where F_p shows a maximum value also decreases with proceeding structural relaxation, i.e. about 0.16 for the as-quenched sample, about 0.12 for the sample annealed at 373 K and about 0.07 for the sample annealed at 473 K. A comparison is made at the same values of the reduced temperature and the reduced magnetic field as shown in Fig. 14, in which F_p values at a reduced temperature $t = T/T_c = 0.84$ were shown as a function of B/H_{c2} for $Zr_{70}Cu_{30}$ alloy in as-quenched and annealed ($T_a = 373\,K$ and $t_a = 1\,h$) states. Annealing results in decreases in the maximum F_p values from 0.52×10^4 to $0.46 \times 10^4\,N\,m^{-3}$ and the value of B/H_{c2} at $F_{p,max}$ from 0.18 to 0.15. These results suggest that the irrecoverable structural relaxation in the amorphous phase causes a decrease of the fluxoid pinning force through an increase in the homogeneity in the amorphous structure on the scale of coherence length ($\simeq 8.7$ nm).

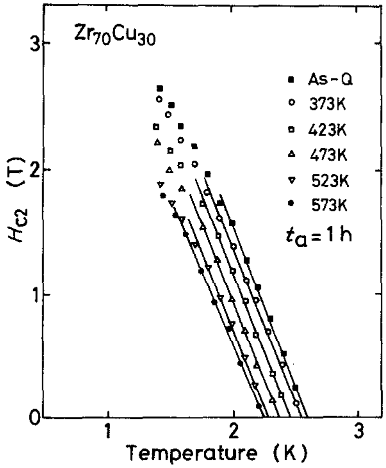

Figure 10 Temperature dependence of upper critical field H_{c2} of an amorphous $Zr_{70}Cu_{30}$ alloy annealed for 1 h at various temperatures from 373 to 523 K.

3.5. Change in normal electrical resistance $R(T)$ upon annealing

The normal electrical resistance of $Zr_{70}Cu_{30}$ amorphous alloy in the as-quenched and annealed states for 100 h at 373 and 523 K was measured in the temperature range from 77 to 250 K and its normalized resistance R/R_{77} is plotted as a function of temperature in Fig. 15. It can be seen that the R/R_{77} value in the range from 150 to 250 K varies almost linearly with temperature. The temperature coefficient of resistivity (TCR) at 250 K, $1/\rho_{250}(\mathrm{d}\rho/\mathrm{d}T)$, is negative and its magnitude decreases with proceeding structural relaxation, e.g. 1.45×10^{-4} for the as-quenched sample, 1.40×10^{-4} for the sample annealed for 100 h at 373 K and 1.23×10^{-4} for the sample annealed for 100 h at 523 K.

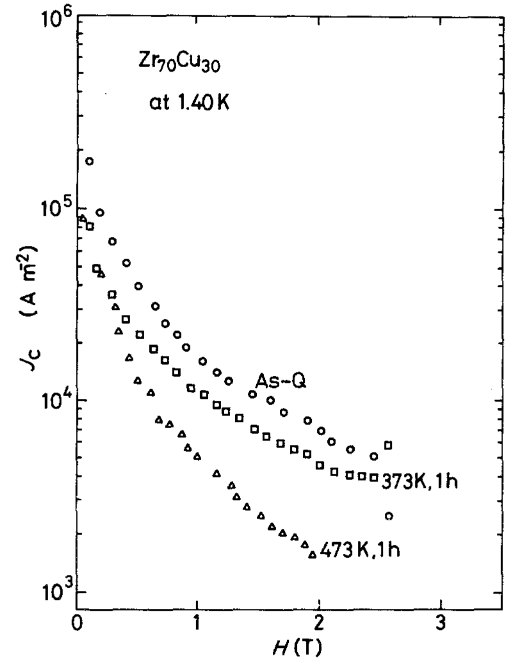

Figure 12 Critical current density, J_c, at 1.40 K as a function of magnetic field of an amorphous $Zr_{70}Cu_{30}$ alloy in the as-quenched and annealed states.

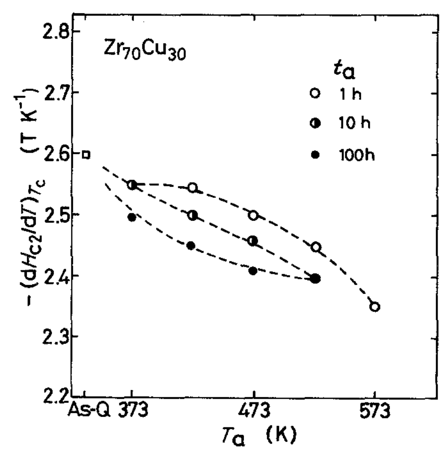

Figure 11 Change in the temperature gradient of H_{c2} near T_c, $-(\mathrm{d}H_{c2}/\mathrm{d}T)_{T_c}$, as a function of annealing temperature for an amorphous $Zr_{70}Cu_{30}$ alloy annealed for 1, 10 and 100 h.

4. Discussion

4.1. Activation energy for irrecoverable structural relaxation

Based on the data of Figs. 1 to 4, the normalized enthalpy relaxation, $\Delta H_{\mathrm{i,exo}}(T_a, t_a)/\Delta H_{\mathrm{i,exo}}(\infty)$,

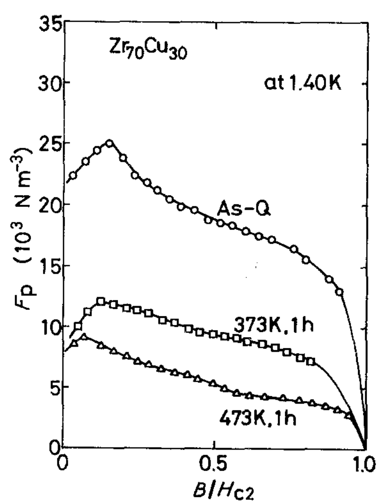

Figure 13 Fluxoid pinning force F_p as a function of reduced magnetic field $b = B/H_{c2}$ for an amorphous $Zr_{70}Cu_{30}$ alloy in the as-quenched and annealed states.

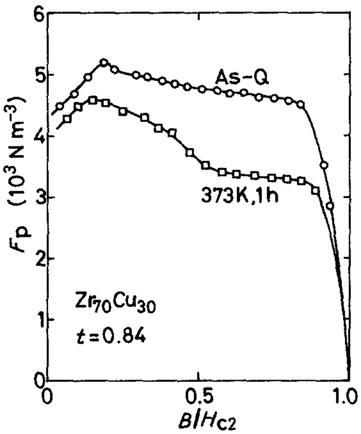

Figure 14 Fluxoid pinning force F_p at the same reduced temperature $t = T/T_c = 0.84$ as a function of reduced magnetic field $b = B/H_{c2}$ for an amorphous $Zr_{70}Cu_{30}$ alloy in as-quenched and annealed states.

as a function of the logarithm of t_a at various T_a is replotted in Fig. 16, where $\Delta H_{i,exo}(\infty)$ is for the as-quenched alloy. $\Delta H_{i,exo}(T_a, t_a)/\Delta H_{i,exo}(\infty)$ scales linearly with log t_a in the temperature range of 373 to 523 K. $\tau_{1/2}$, the annealing time required to reach the midpoint of the irrecoverable relaxation enthalpy at a given T_a, is plotted in Fig. 17 as a function of the inverse of $T_a(1/T_a)$. $\tau_{1/2}$ follows an Arrhenius equation:

$$\tau_{1/2} = \tau_0 \exp(E/k_B T_a) \qquad (3)$$

where E is the activation energy and k_B is the Boltzmann constant. The activation energy determined from the slope in Fig. 17 was found to be 1.5 eV. Assuming a first-order reaction process, the attempted frequency, ν_0, is evaluated to be approximately 6.6×10^{13} sec^{-1}, being nearly the same order as the Debye frequency ($\nu_D \simeq 10^{13}$ to 10^{14} sec^{-1}). This result may allow us to infer that the irrecoverable structural relaxation occurs more or less independently from each other in a noncooperative manner.

Similarly, the ratio of the difference between the superconducting transition temperature of the as-quenched sample, $T_{c,q}$, and that of annealed sample, $T_{c,a}$, $[\Delta T_c(T_a, t_a) = T_{c,q} - T_{c,a}]$ to the largest difference between $T_{c,q}$ and the lowest $T_{c,a}[\Delta T_c(\infty)]$ is plotted as a function of ln t_a at different T_a in Fig. 18 for $Zr_{70}Cu_{30}$. $\Delta T_c(T_a, t_a)/\Delta T_c(\infty)$ varies linearly with ln t_a, similar to the result of the irrecoverable relaxation enthalpy (Fig. 17).

The ln $[\tau_{1/2}(h)]$ at a given T_a is plotted as a function of $1/T_a$ in Fig. 19, where $\tau_{1/2}$ is the annealing time required to reach $0.5\Delta T_c(T_a, t_a)/\Delta T_c(\infty)$. The activation energy determined from the slope in Fig. 18 is about 1.5 eV and the jump frequency (ν_0) over this barrier evaluated from the activation energy is about 1.9×10^{14} sec^{-1}.

The E and ν_0 values obtained from the ratio of the lowering of T_c, $\Delta T_c(T_a, t_a)/\Delta T_c(\infty)$ are in good agreement with those obtained from the irrecoverable relaxation enthalpy. The good agreement of both the E and ν_0 values allows us to conclude that the degradation of T_c on annealing originates from the irrecoverable structural relaxation due to the annihilation of various kinds of quenched-in defects such as voids, vacancies and density fluctuations, etc. as well as the topological and chemical instabilities.

We noted the endothermic reaction which has been considered to correspond to the recoverable relaxation arising from short-range localized relaxation in regions of the more or less rigid matrix [9] does not play a significant role in the degradation

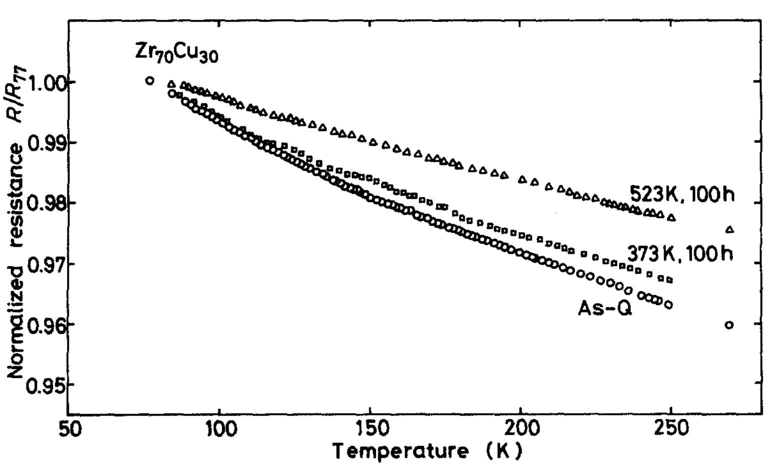

Figure 15 Reduced electrical resistance R/R_{77} as a function of temperature of an amorphous $Zr_{70}Cu_{30}$ alloy in as-quenched and annealed states.

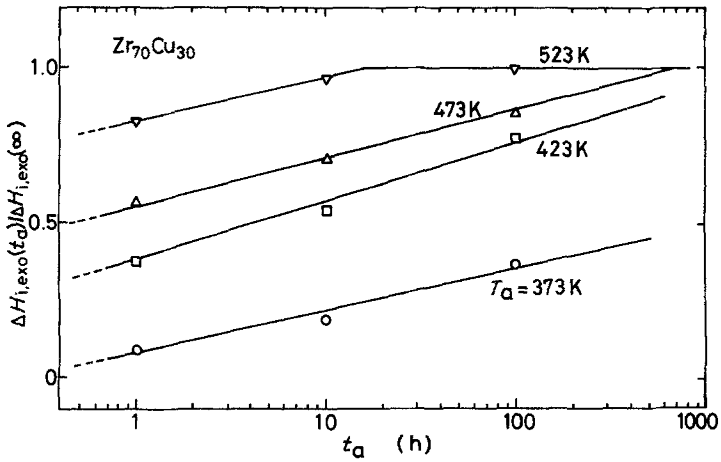

Figure 16 Change in the increasing ratio of the irrecoverable relaxation enthalpy $\Delta H_{i,exo}$ as a function of logarithm of annealing time for an amorphous $Zr_{70}Cu_{30}$ alloy annealed at various temperatures from 373 to 573 K.

of T_c, being consistent with the conclusion derived from the data of the a.c. susceptibility. These conclusions are also supported by the fact that the degradation of T_c always occurs irrecoverably and no recoverable change in T_c is observed for all the amorphous superconductors examined up to date.

4.2. Changes in other superconducting parameters on irrecoverable structural relaxation

In order to clarify the microscopic origin of the depression of T_c by the irrecoverable structural relaxation, the changes in the dominating parameters for T_c upon annealing were investigated for $Zr_{70}Cu_{30}$ amorphous alloy. McMillan's [12] superconducting theory, which is applicable to an intermediate strong-coupling superconductor, states that T_c is dominated by the Debye temperature θ_D and the electron–phonon coupling constant λ; the larger the θ_D and λ the higher the T_c, but the contribution is much larger for λ.

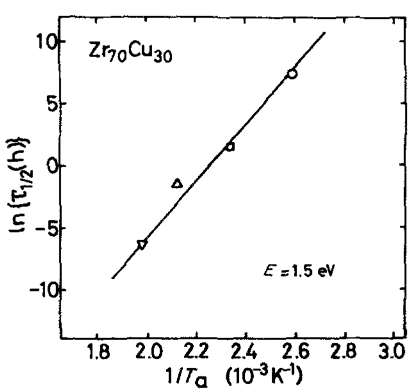

Figure 17 Arrhenius plot for determining the activation energy for the irrecoverable relaxation enthalpy for an amorphous $Zr_{70}Cu_{30}$ alloy.

The electronic dressed density of states at the Fermi level $N^*(E_f) = N(E_f)(1 + \lambda)$ was estimated from the measured values of the H_{c2} gradient near T_c, $-(dH_{c2}/dT)_{T_c}$, and normal electrical resistivity, ρ_n, by using the following expression based on the Ginzburg–Landau–Abrikosov–Gorkov (GLAG) theories (see [13] for example).

$$N(E_f)(1 + \lambda) = -\frac{\pi}{8k_B e\rho_n}\left(\frac{dH_{c2}}{dT}\right)_{T_c} \qquad (4)$$

The formula is applicable in the dirty limit where the electron mean free path is much less than the BCS superconducting coherence length $l \ll \xi_0$. This criterion is well satisfied for the present amorphous superconductor with extremely high electrical resistivity ($\simeq 1.90\,\mu\Omega m$). The values of $N(E_f)(1 + \lambda)$ thus obtained are summarized in Table I, together with the experimental values of T_c, ρ_n and $-(dH_{c2}/dT)_{T_c}$. Additionally, two parameters characterizing the amorphous superconductors of the GL coherence length $\xi_{GL}(0)$ at 0 K and the electronic diffusivity D estimated from an extended GLAG theory are also represented for reference. As seen in Table I, the $N(E_f)(1 + \lambda)$ decreases from 2.50×10^{47} to 2.17×10^{47} states $m^{-3}\,J^{-1}\,spin^{-1}$ with increasing T_a. Fig. 20 shows the correlation between T_c and $N(E_f)(1 + \lambda)$ for a series of $Zr_{70}Cu_{30}$ samples in the as-quenched and annealed states. A correlation that the larger the $N(E_f)(1 + \lambda)$ value the higher the T_c is seen. This suggests that the degradation of T_c by the irrecoverable structural relaxation is interpreted as due to the decrease in λ and/or $N(E_f)$.

The Eliashberg equation, which gives the accurate numerical solution of T_c, describes the relation between the λ and the phonon frequency

TABLE I Superconducting transition temperature T_c, the residual electrical resistivity ρ_n, H_{c2} gradient at T_c – $(dH_{c2}/dT)_{T_c}$, the dressed density of states at the Fermi level $N(E_f)(1 + \lambda)$, the GL coherence length $\xi_{GL}(0)$ and the electronic diffusivity D for $Zr_{70}Cu_{30}$ amorphous alloy in as-quenched and annealed states

T_a(K) × t_a(h)	T_c(K)	ρ_n(μΩm) at 4.2 K	$-(dH_{c2}/dT)_{T_c}$ (T K^{-1})	$N(E_f)(1 + \lambda)$ (10^{47} states m^{-3} J^{-1} spin^{-1})	$\xi_{GL}(0)$ (nm)	D (mm^2 sec^{-1})
As-quenched	2.69	1.85	2.60	2.50	8.2	42
373 × 1	2.56	1.83	2.55	2.48	8.3	43
373 × 10	2.53	1.85	2.55	2.45	8.3	43
373 × 100	2.51	1.86	2.50	2.39	8.4	44
423 × 1	2.39	1.89	2.55	2.40	8.6	43
423 × 10	2.34	1.88	2.50	2.37	8.8	44
423 × 100	2.28	1.86	2.45	2.34	9.0	45
473 × 1	2.32	1.91	2.50	2.33	8.8	44
473 × 1'0	2.29	1.89	2.45	2.26	9.0	46
473 × 100	2.24	1.91	2.40	2.24	9.1	46
523 × 1	2.28	1.94	2.45	2.25	9.0	45
523 × 10	2.26	1.97	2.40	2.17	9.1	46

ω as follows [12]:

$$\lambda = 2\int_0^\infty \alpha^2(\omega)F(\omega)d\omega/\omega \quad (5)$$

Here $F(\omega)$ is the phonon spectrum and $\alpha(\omega)$ is the electron–phonon matrix element. Although there is no information on the change in the quantity $\alpha^2(\omega)F(\omega)$ for an amorphous phase by structural relaxation, the change in λ on annealing can be inferred by using the following McMillan factorization of λ:

$$\lambda = \frac{N(E_f)\langle I^2 \rangle}{M\langle \omega^2 \rangle} \quad (6)$$

where $\langle I^2 \rangle$ is the average over the Fermi surface of the square of the electronic matrix element, M the average ionic mass and $\langle \omega^2 \rangle$ an average of the square of the phonon frequency. There are a number of reports that the irrecoverable structural relaxation of an amorphous phase causes an increase in density by about 0.5% [14] and the Young's modulus sound velocity (V_E) by about 7% [15–17]. Based on the Debye approximation, the V_E is expressed in terms of the Debye phonon frequency ω_D and θ_D as follows [18]:

$$V_E = \frac{k_B\omega_D}{\hbar}\left(\frac{6\pi^2 N}{\Omega}\right)^{-1/3} = \theta_D\left(\frac{6\pi^2 N}{\Omega}\right)^{-1/3} \quad (7)$$

Here N/Ω is the number of atoms per unit volume. Equation 7 clearly indicates that the increase in V_E corresponds to the increase in ω_D and θ_D. In addition, it has been clarified from low-temperature specific-heat measurement [3, 19] that the $N(E_f)(1 + \lambda)$ value of $Zr_{74}Cu_{26}$, $Zr_{70}Cu_{30}$ and $Zr_{64}Cu_{36}$ amorphous alloys decreases by about 3 to 4% on annealing at 423 to 473 K for 10 to 20 h. Accordingly, the decrease in λ by the irrecoverable

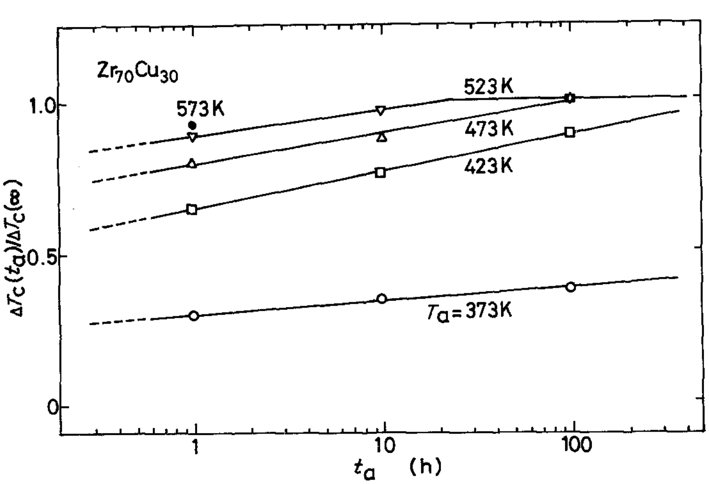

Figure 18 Change in the degradation ratio of T_c as a function of logarithm of annealing time for an amorphous $Zr_{70}Cu_{30}$ alloy annealed at various temperatures from 373 to 573 K.

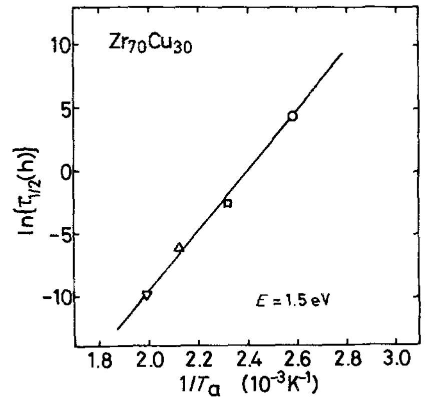

Figure 19 Arrhenius plot for determining the activation energy for the degradation of T_c for an amorphous $Zr_{70}Cu_{30}$ alloy.

structural relaxation is thought to originate from the increase in M and $\langle\omega^2\rangle$ and the decrease in $N(E_f)$, even though the change in $\langle I^2\rangle$ by structural relaxation remains unknown for the present amorphous superconductor. From the above-described discussion, the degradation of T_c by the irrecoverable structural relaxation is inferred to originate from the decrease in λ due to the increase of M and $\langle\omega^2\rangle$ and/or the decrease in $N(E_f)$. This inference is consistent with the previous interpretation [5] for Nb–Zr–Si and Zr–Si amorphous alloys.

Recently, Inoue *et al.* have found the existence of a close correlation between T_c and the electrical residual resistivity ρ_n for superconducting Nb–Zr–Si [20], Zr–Si [21] and Zr–Ge [21] amorphous alloys; the higher the ρ_n the lower the T_c, even though different types of electrons respond for normal electrical resistivity and for superconductivity, s-electrons carry most of the normal state current, whereas the d-electrons are mainly responsible for superconductivity. Such a correlation allows us to entertain the expectation that the strong correlation between T_c and ρ_n might also exist for $Zr_{70}Cu_{30}$ amorphous alloy in as-quenched and relaxed states. Although there is considerable scatter in ρ_n owing to the lack of uniformity in sample form, the ρ_n values summarized in Table I tend to increase slightly with proceeding structural relaxation. The tendency is consistent with the previous data [22, 23] that the irrecoverable structural relaxation of an amorphous phase causes an increase in ρ_n by about 2%. Accordingly, the $Zr_{70}Cu_{30}$ amorphous alloy in as-quenched and annealed states is concluded to have the same tendency that the higher the ρ_n the lower the T_c. Such a close correlation can be qualitatively interpreted by the following simple relation:

$$\rho_n \propto [N(E_f)De^2]^{-1} \qquad (8)$$

The theoretical derivation of a similar correlation $[N(E_f) \propto 1/\rho_n]$ has been presented in the studies of T_c and ρ_n for crystalline Nb_3Ge and niobium film superconductors [24]. Table I shows that the D-value tends to increase slightly with proceeding structural relaxation. Accordingly, Equation 8 allows us to infer that the degradation of T_c and the increase in ρ_n upon structural relaxation arise from the decrease in $N(E_f)$.

Furthermore, it was shown in Fig. 15 that the temperature coefficient of resistivity (TCR) at 250 K, $1/\rho_{250}(d\rho/dT)$, of $Zr_{70}Cu_{30}$ amorphous alloy increased with proceeding structural relaxation for -1.45×10^{-4} in the as-quenched state to -1.23×10^{-4} at $T_a = 423$ K for $t_a = 100$ h, in good contrast to the proportional relation between TCR and λ which has been previously recognized for a number of crystalline superconductors such as Nb_3Ge, niobium, Ag–Ga, Au–Al and Au–Ga [24–27] as well as amorphous Zr–Si and Zr–Ge superconductors [21]. However, if only the absolute value of TCR is taken into consideration, one can notice the existence of the previous proportional relation; the smaller the absolute value of TCR the smaller the λ. This may permit us to interpret that the observed decrease in the absolute value of TCR for $Zr_{70}Cu_{30}$ amorphous alloy by structural relaxation arises from the reduction in λ and the relaxation-induced reduction in λ also causes the degradation of T_c.

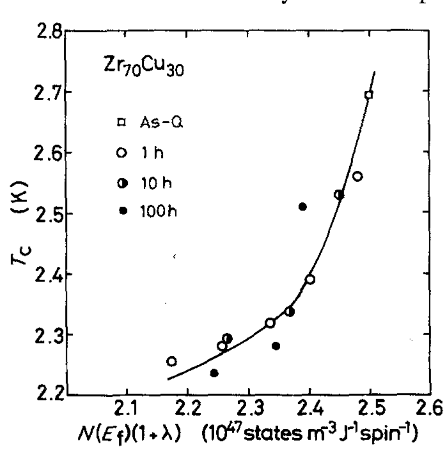

Figure 20 Correlation between T_c and $N(E_f)(1 + \lambda)$ for an amorphous $Zr_{70}Cu_{30}$ alloy in as-quenched and annealed states.

5. Summary

In order to clarify the mutual relation between the structural relaxation enthalpy and the changes in the superconducting properties, the changes in the $C_p(T)$, the relaxation enthalpy, $T_c, H_{c2}(T), J_c(H)$ and F_p upon annealing were examined for $Zr_{70}Cu_{30}$ and $Zr_{70}Ni_{30}$ amorphous alloys by using a differential scanning calorimeter as well as by a conventional four-electrical-probe and Hartshorn bridge techniques. The results obtained are summarized as follows:

1. The irrecoverable structural relaxation on annealing occurs logarithmically with annealing time in the temperature range examined. The activation energy for the irrecoverable relaxation enthalpy was 1.5 eV for $Zr_{70}Cu_{30}$ and the frequency of jump over the barrier was about $6.6 \times 10^{13}\ sec^{-1}$. The irrecoverable relaxation enthalpy is larger by a factor of about 25 than the recoverable relaxation enthalpy.

2. T_c degrades linearly against the logarithm of t_a in the temperature range from 373 to 523 K and the activation energy and the jump frequency for the degradation of T_c are about 1.5 eV and $1.9 \times 10^{14}\ sec^{-1}$, respectively. From the good agreement between the activation energies and the frequencies of jump over the barrier for the increase in $\Delta H_{i,\,exo}$ and the degradation of T_c as well as the invariableness of T_c before and after the recoverable structural relaxation, it is reasonably concluded that the degradation of T_c occurs by the irrecoverable structural relaxation.

3. The dressed density of electronic states at the Fermi level $N(E_f)(1 + \lambda)$ which was calculated from the measured values of ρ_n and $-(dH_{c2}/dT)_{T_c}$ by using the GLAG theories, exhibits an annealing dependence similar to that of T_c. From this correlation, the degradation of T_c by structural relaxation was interpreted as originating from the decrease in λ due to the increase in M and ω as well as the decrease in $N(E_f)$.

4. The $J_c(H)$ and F_p decrease significantly by the irrecoverable structural relaxation as a result of an enhancement of the homogeneity in the amorphous structure on the scale of coherence length due to the annihilation of various kinds of quenched-in defects and the topological and compositional atomic regroupings.

References

1. A. J. DREHMAN and W. L. JOHNSON, *Phys. Status Solidi* (*a*) **52** (1979) 499.
2. A. RAVEX, J. C. LASJAUNIAS and O. BETHOUX, *Physica* **107B** (1981) 397.
3. S. GRONDEY, H. V. LOHNEYSEN, H. J. SCHNIK and K. SAMWER, *Z. Phys.* **B51** (1983) 287.
4. C. C. KOCH, D. M. KROEGER, J. S. LIN, J. O. SCARBROUGH, W. L. JOHNSON and A. C. ANDERSON, *Phys. Rev.* **27** (1983) 1586.
5. A. INOUE, S. OKAMOTO, N. TOYOTA, T. FUKASE, K. MATSUZAKI and T. MASUMOTO, *J. Mater. Sci.* **19** (1984) 2719.
6. T. EGAMI, *Mater. Res. Bull.* **13** (1978) 557.
7. H. S. CHEN and E. COLEMAN, *Appl. Phys. Lett.* **28** (1976) 245.
8. H. S. CHEN, *J. Appl. Phys.* **52** (1981) 1868.
9. *Idem*, *J. Non-Cryst. Solids* **46** (1981) 289.
10. A. INOUE, T. MASUMOTO and H. S. CHEN, *J. Mater. Sci.* **19** (1984) 3953.
11. H. S. CHEN and A. INOUE, *J. Non-Cryst. Solids* **61/62** (1984) 805.
12. W. L. McMILLAN, *Phys. Rev.* **167** (1968) 331.
13. T. P. ORLANDO, E. J. MCNIFF, Jr, S. FORNER and M. R. BEASLEY, *ibid.* **B19** (1979) 4545.
14. H. S. CHEN, J. T. KRAUSE and E. A. SIGETY, *J. Non-Cryst. Solids* **13** (1972/73) 321.
15. H. S. CHEN, *J. Appl. Phys.* **49** (1978) 3289.
16. A. KURSUMOVIC, M. G. SCOTT, E. GIRT and R. W. CAHN, *Scripta Metall.* **14** (1980) 1303.
17. B. FOGARASSY, A. BOHOYEI, A. CZIRAKI, I. SZABO, Gy. FAIGEL, L. GRANASY, T. KEMENY and I. VINCZE, *J. Non-Cryst. Solids* **61/62** (1984) 907.
18. T. OTSUKA, "Ferroelectrics and Superconductor," edited by the Japan Institute of Metals (Japan Institute of Metals, Sendai, 1973) p. 131.
19. P. GAROCHE, Y. CALVAYRAC, W. CHENG and J. J. VEYSSIE, *J. Phys.* **F12** (1982) 2783.
20. A. INOUE, Y. TAKAHASHI, N. TOYOTA, T. FUKASE and T. MASUMOTO, *J. Mater. Sci* **18** (1983) 114.
21. A. INOUE, T. MASUMOTO and H. S. CHEN, *J. Phys. F:Met. Phys.* **13** (1983) 2603.
22. M. BALANZAT, *Scripta Metall.* **14** (1980) 173.
23. M. BALANZAT, C. MAIVY and J. HILLARET, *J. Phys.* c-**8** (1980) 871.
24. H. LUTZ, H. WEISMANN, M. GURVITCH, A. GOLAND, O. F. KAMMERER and M. STRONGIN, "Superconductivity in d- and f-band Metals," edited by D. H. Douglass (Plenum, New York, 1976) p. 535.
25. L. R. TESTARDI, *IEEE Trans. Magn* **MAG-11** (1975) 197.
26. J. M. POATE, L. R. TESTARDI, A. R. STORM and AUGUSTYNIAK, *Phys. Rev. Lett.* **35** (1975) 1290.
27. O. RAPPAND and M. FLODIN, *Phys. Rev.* **B26** (1982) 99.

Received 23 May and accepted 4 June 1984